PORT SAID ENGINEERING RESEARCH JOURNAL
Faculty of Engineering - Port Said University
Volume 27 No. 4 pp: 40:54

# The Efficiency of By-Product- Based Geo-Polymer Concrete

*Wegdan W. ElNadoury*

*Civil, Department, Faculty of Engineering, Horus University, New Damietta, Egypt, email: wegdanelnadoury@gmail.com*

*DOI: 10.21608/PSERJ.2023.229805.1257*

*Received 19-8-2023*
*Revised 22-9-2023*
*Accepted 16-10-2023*



## ABSTRACT

Geo-polymer concrete (GPC) and industrial byproducts have developed expeditiously as eco-benevolent substitutes for OPC. Whereas elevated curing temperature is essential. This research studies the applicability of producing byproduct-based GPC cured under ambient temperature. The effect of the incorporation of ceramic squander powder (CSP) and rice husk ash (RHA) is assessed. All the investigated mixtures contain 40% Slag, 10% fly ash (FA), and a 50% combination of CSP and RHA. Four different combinations of CSP/RHA; 10/40, 20/30, 30/20, and 40/10 are utilized. w/b ratios; 0.3, 0.4, and 0.45 are tested. Compressive, splitting tensile, and flexural strengths are examined as indicators of mechanical properties. Acid resistance, water absorption, sorptivity, and chloride permeability are evaluated as indicators of durability aspects. The results revealed that the 30/20 combination is optimum in terms of mechanical properties, while all combinations attained applicable durable properties compared to the control mix with 90% slag and 10% FA.

**Keywords**: Geopolymer concrete, Alkali-activated binder, Activation solution, Ceramic powder, Rice husk ash, Eco-friendly concrete

## 1 INTRODUCTION

Landfills for solid squander will resume increasing due to the constantly developing global population and the desire to satisfy consumer wants. The fabrication of ceramic tiles creates ceramic squander powder (CSP) amid the polishing phase[1]. The worldwide era of CSP surpasses twenty-two Billion tons. Getting rid of CSP is considered a challenge, especially for its environmental effect [2]. Waste management is therefore more essential for the development of ecological sustainability. Large-scale solid waste conversion into an alternative resource will assist in addressing environmental and landfill overflow issues while minimizing the need for nonrenewable resources of materials and energy [3]. Researchers [4-6] are looking into novel solid waste materials and their potential for recycling into new goods.

Concrete, the most used man-made element, has generated substantial interest as a potential means of recycling solid waste, particularly those that can replace cement, a key source of greenhouse gas emissions [7,8]. The fabrication of OPC results in a high quantity of $CO_2$ [9]. About 5-8% of the yearly greenhouse gas emitted into the environment worldwide comes from the cement sector [10]. During the last decades, researchers [11–14] investigated the substitution of cement by either byproducts or natural pozzolanic materials. Results reveal the ability of substitutional cement materials (SCMs) in to enhance durability and lowering the heat of hydration [15–18]. In addition, the incorporation of pozzolanic materials produces mixtures with low calcium hydroxide, thus improving resistance to chemical attacks [19–21].

Geopolymer concrete (GPC) is a member of a broad class of Alkali Activated Binders as shown in Figure 1[22]. It is a prospective alternative to OPC concrete to diminish carbon discharged during cement production [23-24]. It depends on the reaction of aluminosilicate with an alkaline solution producing a hardened product [25-27]. The synthesis of GPC involved the addition of byproducts [28, 29]. The properties of the manufactured concrete depend on several factors including the form of alkaline activators, the curing temp., and the source of precursor [25,30]. Tailor-made GPC mixtures could have superior properties depending on their constituents [31]. Khater [32] postulated that GPC cured at high temperatures has exceptional strength and thermal constancy properties. Bernal et al [33] proved the lower

rates of chloride permeability for GPC. This agrees with Adam [34] who stated that both chloride permeability and sorptivity are improved. This is certified to the increase in the concentration of the alkaline-activated binder. El-Feky et al. [35] suggested that mixtures with FA decrease the drying shrinkage. On the contrary, Rashad [36] stated that the GPC mixtures with blended slag and FA raise the drying-shrinkage with an increase in the percentage of slag added. Kim et al. [37] postulated that the usage of Rice Husk Ash (RHA) plus $Na_2SiO_3$ and NaOH improves both the acid and sulfate resistance.

the utilization of CSP as a fractional substitution of cement was studied by some analysts [38-40]. The supreme result was that CSP exhibited pozzolanic action after 28 days. Although the prompt compressive strength was diminished via the incorporation of CSP [40], the durability of mixtures was improved by the addition of CSP [38]. Huseien et al. [41] used CSP in self-compacting concrete, they debated that CSP decreases the probability of segregation and increases the flowability. Aly et al. [42], Azevedo et al. [43], and Saxena and Gupta [44] considered the consequence of excessive temperature curing, 60 °C, on the strength of CSP/Slag blended mixtures. The mixtures achieved less than 40 MPa in strength. They suggested 5% of CSP as an optimum %. Rashad and Essa [45] and Zhang et al. [46] examined samples of CSP/Slag cured under 45°C, they suggested the worthy effect of CSP. Shoaei et al. [47] achieved a strength of 27.5 MPa for samples cured at 105 °C.

All previous studies applied heat curing for CSP/slag mixtures which restricted the utilization of GPC. So far, the inclusion of CSP as a FA substitution in GPC cured at ambient temperatures has not been reported. A comprehensive analysis to deliberate the utilization of CSP within the manufacture of GPC is required. This paper provides an assessment of the durability and mechanical properties of blended mixtures with diverse ratios of CSP and RHA, in addition to slag, and FA.

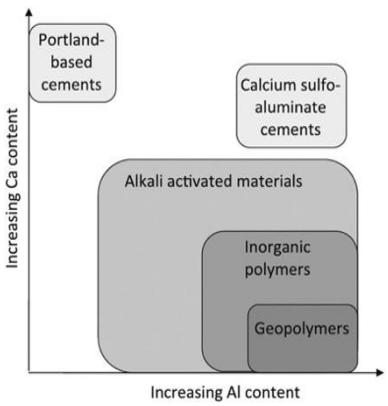


**Figure 1: Alkali-activated materials classification [22].**

## 2 SIGNIFICANCE

The concrete industry is currently dedicated to the production of sustainable concrete by using industrial by-products as a fractional replacement for cement. The use of industrial wastes in geopolymer concrete helps waste disposal and endorses the production of eco-friendly concrete. Fly ash-based geopolymer and slag-based geopolymer had been used previously and considered substitutes for Portland cement due to their availability and low $CO_2$ emissions. However, the elevated curing temperature required for this concrete hinders their wide applications. The research aims to assess the potential of recycling ceramic waste powder and Rice husk ash as a geopolymer binder. Thus provides an ecological method for the disposal of both CSP and RHA. Moreover, the paper evaluates the applicability of producing geopolymer concrete under ambient temperature. Consequently, overcomes the limitations of the broad usage of geopolymer concrete.

## 3 METHODOLOGY

This research is designed to generate superior-strength GPC as a sustainable material integrating byproducts; CSP and RHA in diverse percentages to lessen $CO_2$ emission amid the cement industry. The investigation includes microstructure investigation, durability aspects, mechanical properties, and the effect of the curing regime on GPC. Four water-binder ratios; 0.25, 0.3, 0.4, and 0.45 were experimented to represent a broad range of frequently applied mixtures.

## 4 EXPERIMENTAL WORK

### 4.1 Materials

#### 4.1.1 Characteristics of CSP

Because the water was used throughout the polishing process, the ceramic waste produced was moist. 36% of the bulk of the material was moisture. The air-permeability was tested using a Blaine air permeability device. The average specific surface area (SSA) was 570 m2/kg. In addition, around 45% of the CSP particles, measured by volume, were between 5-10 µm in size. According to the SEM image in Figure 2, the CSP was composed of angular and irregular particles that resembled cement particles in shape. The majority of CSP is made up of SiO2 and Al2O3. This was confirmed by the chemical analysis determined by XRF as presented in Table 1. About 85% of the bulk of the substance is made up of both oxides which meet the ASTM C618 standard [48] of >70% for natural pozzolana. Additionally, the SO3 and loss on ignition (L.O.I.) met ASTM C618 [48] specifications.

#### 4.1.2 RHA

RHA was achieved from neighboring companies. It was produced under controlled combustion (burning temperatures in the range of 500°C–700°C for a period of about 1 hour. Ninety-seven % passed the 90μ sieve. RHA comprises primarily SiO2, circa eighty-two % of the whole structure. This satisfies the constriction of the ASTM C618[48], see Table 1.

**Table 1. Chemical composition.**

| Material | FA(F) | Slag | RHA | CSP |
|---|---|---|---|---|
| $SiO_2$ | 49.99 | 37.50 | 89.34 | 70.10 |
| $Fe_2O_3$ | 9.00 | 0.73 | 0.40 | 0.56 |
| $Al_2O_3$ | 29.00 | 7.27 | 0.45 | 12.2 |
| MgO | 1.49 | 10.86 | 0.49 | 0.99 |
| CaO | 2.38 | 38.48 | 0.76 | 0.02 |
| $Na_2O_3$ | 0.83 | 0.64 | - | 13.46 |
| $SO_3$ | 0.29 | 0.39 | 0.90 | - |
| $P_2O_5$ | - | - | 2.58 | - |
| $K_2O$ | 2.41 | 0.26 | 4.98 | 0.03 |
| L.O.I | 4.00 | 2.13 | - | 0.13 |

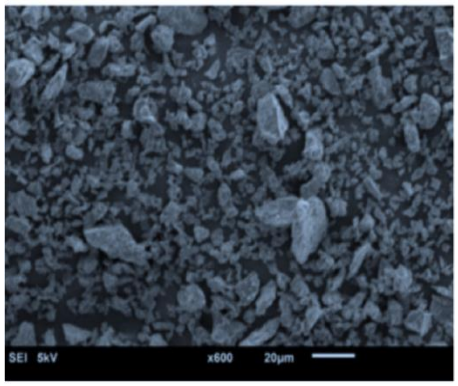


**Figure 2: SEM for CSP.**

#### 4.1.3 Fly Ash

A combination of sodium hydroxide (SH) (14M) and sodium silicate (SS) ($Na_2O$ = 17%, $SiO_2$ = 36%, and water = 47% by mass) with SS/SH of 0.75 was adopted.

#### 4.1.4 Aggregates

Commercially available crushed stone with a N.M.S. of 19 mm was utilized. Local natural sand was utilized as fine aggregate, see Table 2.

**Table 2. Physical properties.**

| Property | Fine | Coarse | CSP | RHA | FA | Slag |
|---|---|---|---|---|---|---|
| Sp. Gr. | 2.64 | 2.72 | 2.3 | 2.08 | 2.62 | 2.09 |
| Fineness M. | 2.53 | 2.76 | 12.2 | 0.695 | 2.96 | 3.27 |
| W. Absorption | 1.8% | 2.1% | ----- | ----- | ----- | ----- |
| Crushing V. | ---- | 20.6% | ----- | ------ | ----- | ----- |

### 4.2 Mixture proportions

Twenty mixtures blended with different percentages of CSP and RHA were prepared. A mixture with a precursor blend of GGBS/FA equals 90/10 is used as the control mix. In all other mixtures, the precursor was a blend of (GGBA+ FA)/ (CSP + RHA) fixed at 50/50. The percentage of GGBS and FA were kept constant at 40% and 10 %, respectively. Whereas the percentage of CWP and RHA differs as follows; 10CWP+ 40 RHA, 20 CWP + 30 RHA, 30 CWP + 20 RHA, and 40 CWP + 10 RHA. A detailed description of the mixes is given in Table 3.

### 4.3 Curing regime

Specimens required for different tests are cast and then de-molded after 24 hours. To assess the applicability of producing efficient GPC cured under ambient temperature, three curing regimes were applied. The two regimes differ in the temperature applied for the first 24 hours of curing namely, ambient temperature, and 100ºC. For achieving 100 ºC curing, the specimens were kept in the oven for 1hr. All specimens are then cured in air for more 27 days.

### 4.4 Test Procedures

#### 4.4.1 Setting time

Detecting initial and final settings is a crucial property. The test is conducted to fulfill ASTM C125[49].

#### 4.4.2 Workability

It is a vital factor for evaluating the easiness and consistency of the fresh mixture. The test was measured by slump fulfilling ASTM C143[50].

#### 4.4.3 Mechanical properties of GPC

*A. Compressive strength*

GPC eternally demonstrates quite higher early strength. It can achieve up to 60 MPa on 1st day and more than 100 MPa on 365 days [51]. Twelve 150 mm cubes were cast per mix. The uncertainty = ± 0.04 mm. Specimens were cured in the three different regimes mentioned in section 3.3 and were tested at 3, 28, and 56 days. Outcomes are approximated to the closest 0.1N/mm.

*B. Tensile Strength*

Sixty cylindered specimens 150 x 300 mm undergo tensile strength test. The average of 3 specimens from each mixture examined per ASTM C496/C496M [52] was noted. Flexural Strength Specimens assessed conferring to ASTM C78/C78M [53] by 3-points loading. The average of 3-beams was calculated.

**Table 3. Mixture Proportions**

| Mix | F. agg. | C. agg. | CSP (kg/m$^3$) | RHA (kg/m$^3$) | Slag (kg/m$^3$) | FA (kg/m$^3$) | NaOH | | Sodium Silicate | Water added | Slump (mm) | Water absorption % | |
|---|---|---|---|---|---|---|---|---|---|---|---|---|---|
| | | | | | | | Mass | Molarity | | | | Tap | Boiled |
| AC0R0 | 561 | 1309 | 0 | 0 | 513 | 57 | 35 | 14 | 88 | 16.5 | 80 | 3.5 | 4.05 |
| AC10R40 | 561 | 1309 | 57 | 228 | 228 | 57 | 35 | 14 | 88 | 16.5 | 82 | 3.52 | 4.11 |
| AC20R30 | 561 | 1308 | 114 | 171 | 228 | 57 | 35 | 14 | 88 | 16.5 | 84 | 3.6 | 4.25 |
| AC30R20 | 561 | 1309 | 171 | 114 | 228 | 57 | 35 | 14 | 88 | 16.5 | 85.6 | 3.64 | 4.30 |
| AC40R10 | 561 | 1309 | 228 | 57 | 228 | 57 | 35 | 14 | 88 | 16.5 | 88 | 3.8 | 4.32 |
| BC0R0 | 670 | 1201 | 0 | 0 | 228 | 57 | 41 | 14 | 103 | 10.3 | 80 | 3.8 | 4.25 |
| BC10R40 | 670 | 1201 | 57 | 228 | 228 | 57 | 41 | 14 | 103 | 10.3 | 82 | 3.83 | 4.30 |
| BC20R30 | 670 | 1201 | 114 | 171 | 228 | 57 | 41 | 14 | 103 | 10.3 | 84 | 3.89 | 4.38 |
| BC30R20 | 670 | 1201 | 171 | 114 | 228 | 57 | 41 | 14 | 103 | 10.3 | 85.6 | 4 | 4.45 |
| BC40R10 | 670 | 1201 | 228 | 57 | 228 | 57 | 41 | 14 | 103 | 10.3 | 88 | 4.2 | 4.49 |
| CC0R0 | 554 | 1294 | 0 | 0 | 228 | 57 | 51 | 14 | 103 | 20.7 | 160 | 4 | 4.37 |
| CC10R40 | 554 | 1294 | 57 | 228 | 228 | 57 | 51 | 14 | 103 | 20.7 | 165 | 4.09 | 4.40 |
| CC20R30 | 554 | 1294 | 114 | 171 | 228 | 57 | 51 | 14 | 103 | 20.7 | 168 | 4.15 | 4.45 |
| CC30R20 | 554 | 1294 | 171 | 114 | 228 | 57 | 51 | 14 | 103 | 20.7 | 171 | 4.25 | 4.56 |
| CC40R10 | 554 | 1294 | 228 | 57 | 228 | 57 | 51 | 14 | 103 | 20.7 | 174.5 | 4.3 | 4.8 |

#### 4.4.4 Durability Properties of GPC

*A. Sorptivity*

The test is conducted to fulfill ASTM C1585[54]. The samples were kept at a (50 ± 2) °C temperature and 80 ± 3% RH for 3-days then for 15-days in sealable containers. Sorptivity is calculated from the slope of a linear relation of absorption (I) and the $\sqrt{time}$, Equation (1).

$$I = \Delta m/(Axg) \quad (1)$$

Where m is the change in specimen mass in grams,
A is the exposed area of the specimen in mm$^2$,
g is the density of water in grams/mm$^3$

*B. Water absorption (W.A.)*

W.A. was examined using the ASTM C642–13 [55]. The specimens were immersed in water for 2 days at 23 °C after being oven-dried for 24h at 110 °C. Equation (2) was utilized to calculate the W.A. Samples were then kept in boiling water for five hours and then left to cool for 15 h to reach 23 °C. The water absorption was calculated using Equation (3).

$$\text{Water absorption} = [(w_1 - w_0)/w_0] * 100 \quad (2)$$

$$\text{Water absorption} = [(w_2 - w_0)/w_0] * 100 \quad (3)$$

Where $w_0$ is the dry weight,
$w_1$ is the saturated weight,
$w_2$ is saturated weight of the boiled specimen.

*C. Chloride permeability*

The test is conducted in accordance to ASTM 1202-97[56].

*D. Carbonation*

The test detects the depth of carbonation using a phenolphthalein solution. Specimens were tested 365 days after casting. Each specimen is sprayed with a 0.2% solution of phenolphthalein to distinguish the loss of alkalinity.

*E. Drying shrinkage*

It is correlated to the loss of moisture from the concrete. It was proceeded in line with ASTM C596-09[57]. The % of shrinkage was considered using Equation (4).

$$\% \text{ of shrinkage} = (Lo - L)/Lo \times 100 \quad (4)$$

where, Lo is starting-length and L is new-Length (mm)

*F. Acid resistance*

100 mm cubes were set to assess the sulfuric and hydrochloric acid resistance. After curing, these cubes were submerged in 5% concentrated sulphuric acid and hydrochloric acid solutions at room temperature. The % of weight-loss and CS loss was computed after 28 and 100 days.

## 5 RESULTS AND DISCUSSION

### 5.1 Workability

Table 3 presents the slump for all mixtures. The workability of GPC is slightly influenced by the % of CSP added, exhibiting a rising tendency as the% of CSP increased. This is accredited to the excessive angular shape of the slag compared to CSP. The slump was increased by the range of 3%, 5%, 7%, and 9% for mixes with 10, 20, 30, and 40% CSP respectively. These results are slightly lower than what Huseien et al. [58] revealed,

they found that the addition of CSP to GPC by 50% increases the average diameter in the flow test by 25% compared to the mix with 0% CSP. The variance in results may be attributed to the presence of RHA which is acknowledged by its influence on reducing the workability. On the contrary, the results were opposed by Rashad, A. M. and Essa, G. M. F. and Saxena, R. and Gupta, T. [45, 44] who declared that CSP has a negative effect on workability.

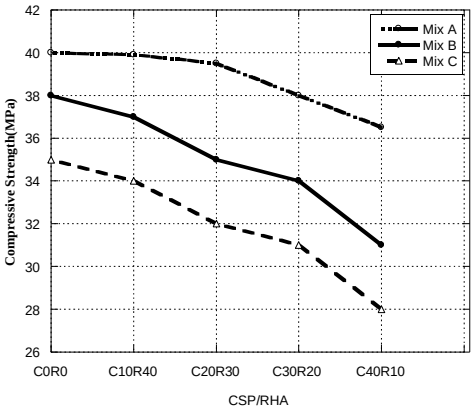


**Figure 3: Compressive strength at 3-days**

### 5.2 Compressive Strength (CS)

Figure 3 illustrates the compressive strength for all mixtures at 3 days. It is perceived that the peak compressive strength is 40 MPa. The lesser CaO content in CSP delayed the formation of C-A-S-H gel which in turn lessened the early compressive strength. On the contrary, outcomes at 28 and 56 days showed that the compressive strength improves with time, see Figure 4. The increase rates in strength were nearly 125, 150, 195, and 170 % for mixes with 10, 20, 30, and 40% CSP at 28 days. Mixtures with 30% CSP+20 % RHA accomplished the peak compressive strength. Both CSP and RHA are rich in silica, increasing the active silica enhances the creation of C-A-S-H gels. The active silica improves the GPC progression and provides extra silicon in the polymer-chain, hence developing the later strength. This is coherent with the previous results [59-62]. Hwang et al. [63] postulate that the existence of Ca+, Si4+, and Al3+ ions in CSP-based GPC produces microstructures rich in C-S-H and C-A-S-H gel. However, Rashad, A.M., and Essa. G.M.F. [45] declared that increasing CSP from 50% to 70 % decreases the compressive strength by 50% due to the diminution in CaO content and the increase in silica. Thus, it could be concluded that using CSP+RHA with a percentage up to 50% will produce high-strength GPC. Higher ratios of CSP+RHA should be studied but Figure 5 presents the impact of curing-temp. on the compressive strength of chosen mixtures. It could be noted that subjecting the specimens to a higher temperature, 100 ºC increased the compressive strength compared to specimens cured at ambient-temperature, however specimens cured at ambient temperature achieved high-strength. This implies that using CSP+RHA-based GPC with SH/SS alkaline activator produces high-strength concrete without special curing conditions according to this research the optimum mix is 30% CSP and 20% RHA.

### 5.3 Tensile Strength

Tensile splitting strength was evaluated at 28 days as shown in Figure 6. It is observed that mixtures BC20R30 and BC30R20 achieved the highest splitting tensile strength, 6.33 MPa. For all groups, mixtures with 10 and 40 % attained the least strength. It is observed that a higher % of CSP than 30% lowers the strength. This is a covenant with Bouaissi et. al[64], and P.S. Deb et. al [65] who declared that a rising quantity of CSP than 50 % directed to the attenuation of calcium and lessened the C-S-H gel. Huseien et al. [58] postulated that using 70% CSP reduces the strength by 60 % compared to mixtures with 50% CSP. Achak et al. [66] exaggerate the effect of CSP on the strength, they postulate that the enhancement at 7 days was boosted by 17% higher than the controlled specimens.

### 5.4 Flexural Strength

The results are demonstrated in Figure 7. Mixtures with 20%CSP/30% RHA attained higher flexural strength for all w/b ratios. Increasing the CSP beyond 30% decreases the results compared to control mixtures. The minimum value was 10 MPa for 40%CSP/10%RHA. The percentage of reduction is slightly lower than that attained by Huseien et al. [58] who stated that flexural strength decreased by 70% on the usage of 70% CSP instead of 50%.

### 5.5 Chloride permeability

A rapid chloride permeability test was applied on all mixtures at 7 and 28-days. At 7-days, the chloride permeability rises as the % of CSP increases, see Figure 8. This is ascribed to the higher porosity of the microstructure. However, at 28 days all mixtures with the same w/b attained nearly the same chloride permeability compared to control mixes with 90% slag. Bernal et al. [35] suggested that the charge passed decreased with a rising % of substitution. This contradicts the results of Visairo et al. [67] who declared that the chloride permeability increases with the increase in % of CSP. The difference in results could be related to the porosity of mixtures. The presence of RHA decreases the porosity of all mixtures compared to mixtures with only CSP.

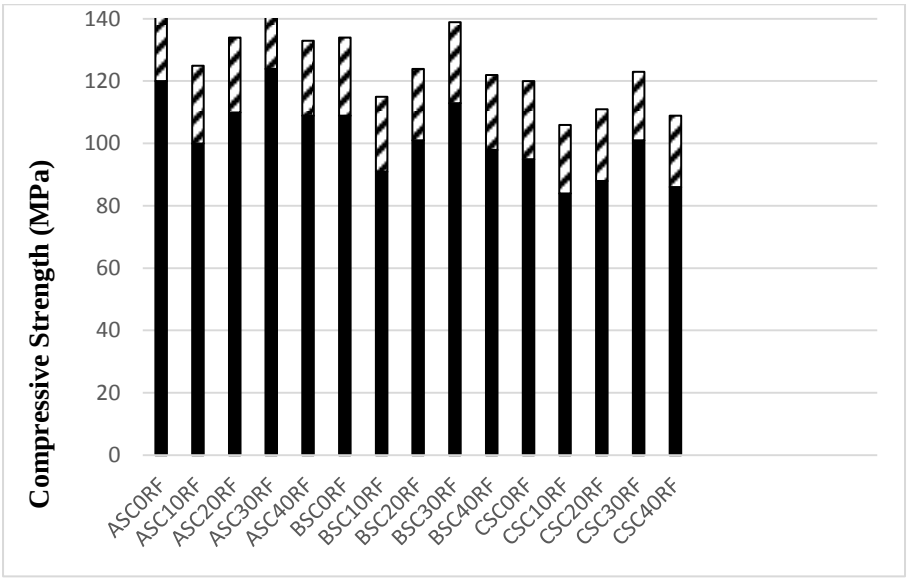


**Figure 4: Compressive strength at 28 and increase in compressive strength 56-days.**

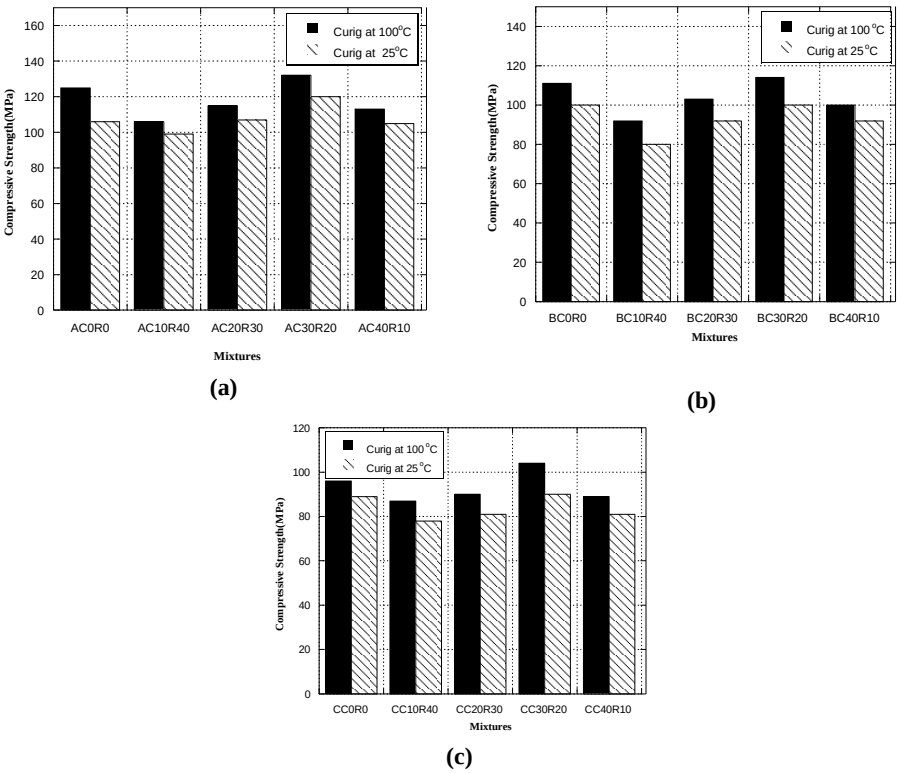


**Figure 5: Influence of curing regime at 28-days, (a) Mix A, (b) Mix B, (c) Mix C**

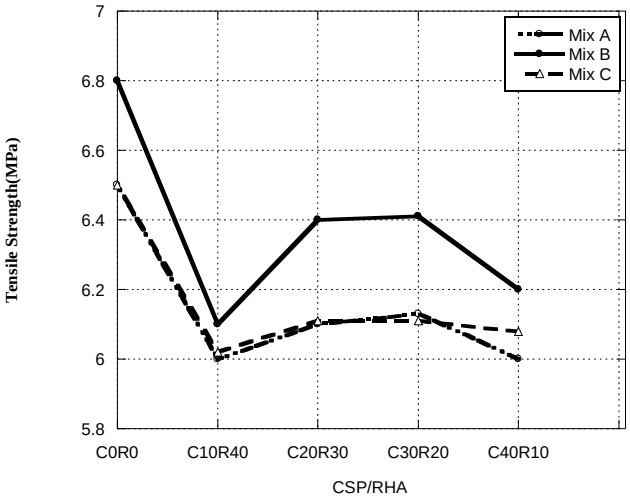


**Figure 6: Tensile strength at 28-days**

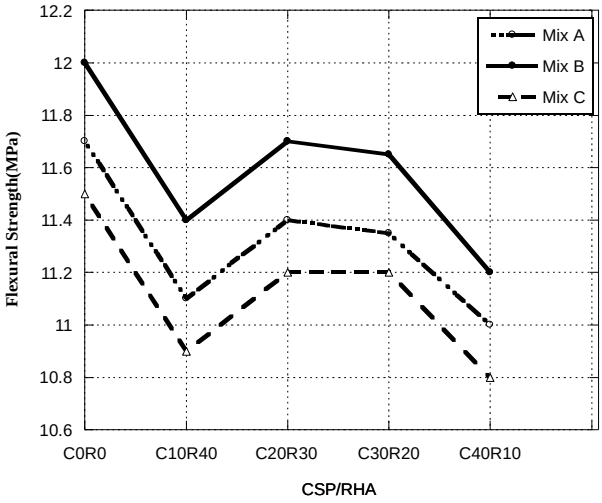


**Figure 7: Flexural strength at 28-days**

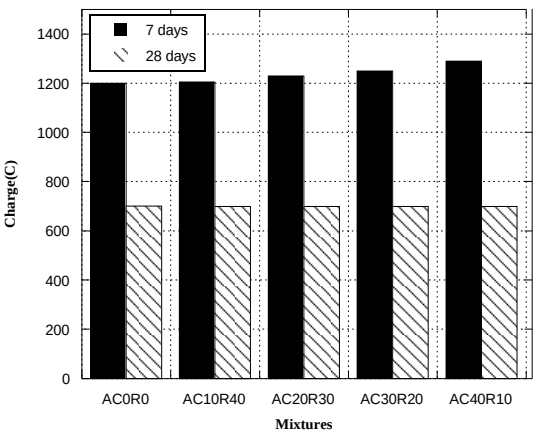


**(a)**

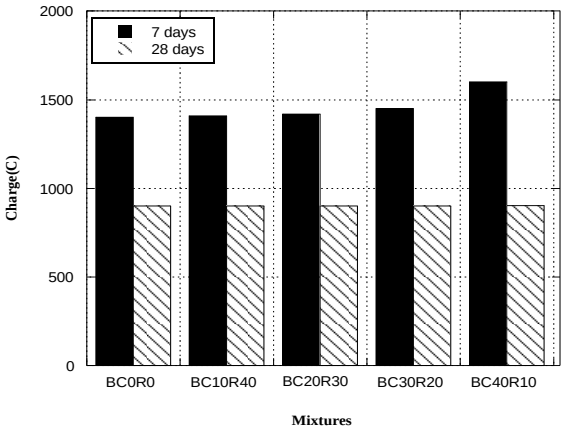


**(b)**

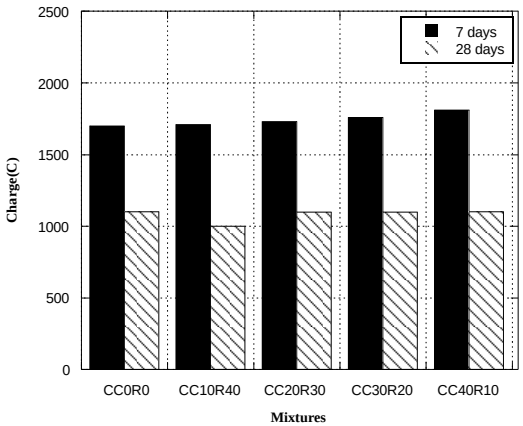


**(c)**

**Figure 8: Chloride permeability at 7 and 28 days, (a) mixA, (b) mix B, (c)mix C**

### 5.6 Water Absorption

This study indicated that water absorption increased with increasing CSP compared to the reference mix, see Table 3. However, all mixtures attained water absorption of less than 4.5% and 5% after being immersed in water at standard temperature and boiling water respectively. These results are in covenant with Huseien et. al [58]and Saxena, R. and Gupta, T [44]

### 5.7 Sorptivity

Figure 9 shows the sorptivity for all mixtures. It is clear that the increase in CSP percentage decreases the sorptivity of the mixture. This is accredited to the effect of the reactivity CSP on the pore-structure. The results confirmed the previous studies of Aly et al. [42] who reported lower sorptivity at 100% CSP compared to mortars with 60% CSP and 40% GGBS. Results also comply with Chen, X. et. al [39] who assumed that CSP improves the impermeability of the concrete. The values for all mixtures < 1, this indicates that all mixtures have excellent to good sorptivity according to the index proposed by Aziz et al. [68].

### 5.8 Carbonation

Figure 10 presents the carbonation depth for all tested mixtures. It is noticed that the carbonation depth for all mixtures is in the range of 3.0 to 5.5 mm. Thus the blind CSP + RHA has no deteriorative effect on GPC compared to slag-based GPC. The results are lower than observed by Zhang et al. [72] who postulate that a carbonation depth of 10mm was observed for GPC with FA. Also, Huseien et al. [71] state that GPC with 10% FA reached a carbonation depth of 7.1 mm. The low penetration depth in this study can be ascribed to the Pozzolanic activity of CSP and RHA which prohibits the diffusion of carbon dioxide in the specimens. These results emphasize results obtained by Bernal et al. [33] who observed highly polymerized alumino-silicate gels in the GPC samples, thus the production of low-emission concrete.

### 5.9 Setting time

Figure 11 shows the initial and final setting time for all mixtures. It is noted that the greater the CSP content, the longer the time required for setting. However, all specimens show higher times compared to control mixes (slag 90%+10 FA). This may be credited to the presence of slag and FA. The incorporation of slag reduces the setting time due to the rise in the Ca content in the mixtures. Whereas the FA reduces the setting times because of its superior surface area compared to cement. The maximum initial and final setting times were 30, and 120 minutes respectively. These results emphasize the previous results [69,70]. Huseien et al. [71] stated that CSP has a determinantal effect on Setting time, 92 min was recorded by mortars with 70% CSP compared to 15 min for mortars with 0% CSP.

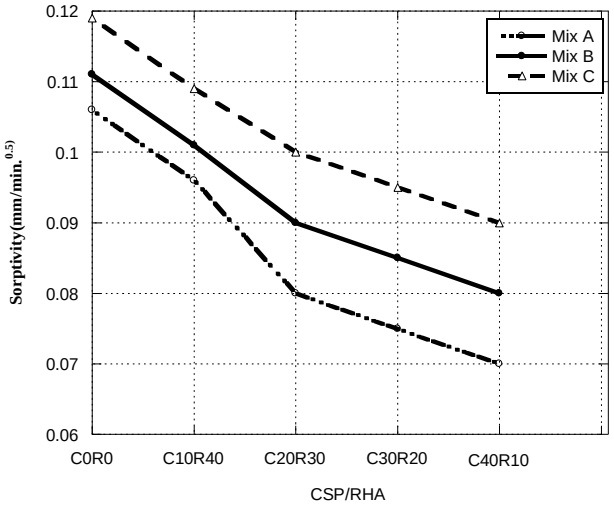


**Figure 9: Sorptivity of mixtures**

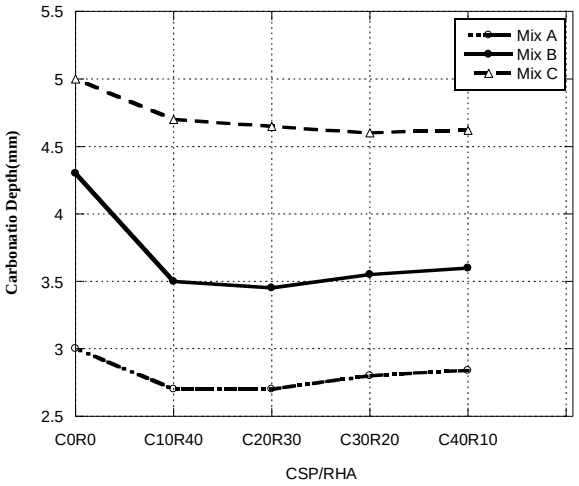


**Figure 10: Carbonation depth (mm)**

### 5.10 Drying Shrinkage

Results proved that blinded GPC mixtures attained lower drying shrinkage than those mixed with slag-based GPC. As shown in Figure 12, the increase in the CSP/ Slag ratio reduced the drying shrinkage. This agrees with Chen et al. [38] and Rashad [36].

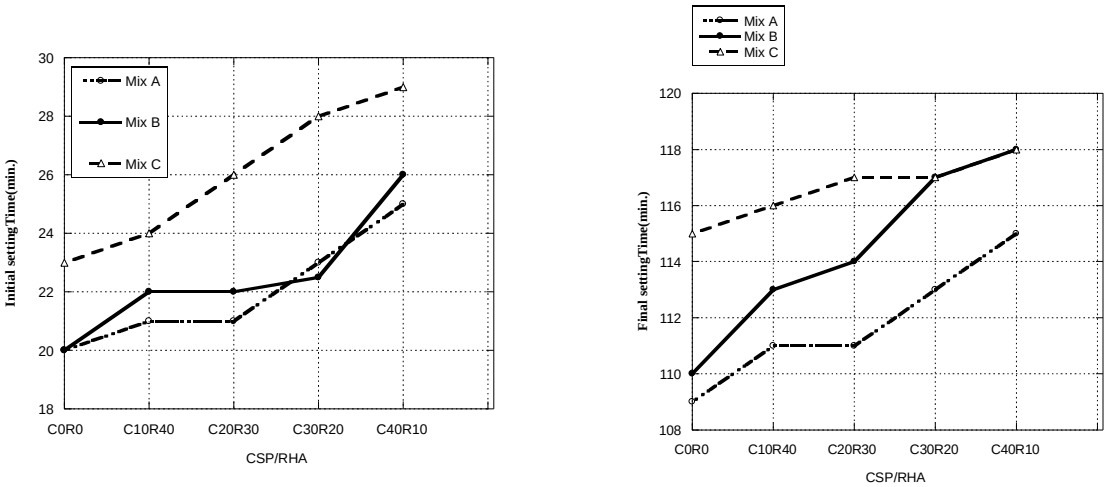


**(a)** **(b)**

**Figure 11: (a) Initial setting time, (b) Final setting time**

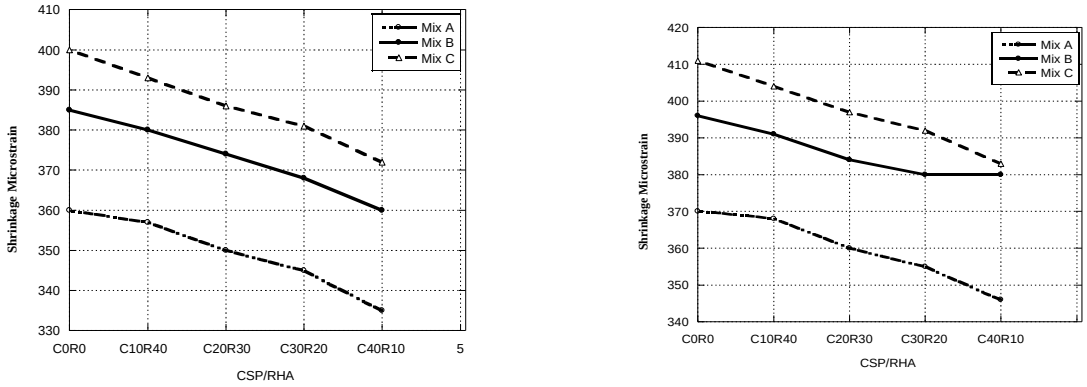


**(a)** **(b)**

**Figure 12: Drying shrinkage of GPC with different CSP/RHA percentages, (a) at 28 days, (b) at 180 days**

### 5.11 Acid Resistance

Specimens are tested after 28 and 180 days of immersion in H2SO4 solutions. Results showed that all mixtures attained an increase in mass at 28 days and then a decrease in mass at 180 days. This is ascribed to the dissolution that occurred due to hydrogen ions and at the same time the formation of gypsum due to the reaction of sulfate and Ca ions. The net effect eventually was the mass loss at 180 days. This complies with Shagnay et al. [73] who indicated that slag improves the resistance of acid.

Malviya and Goliya [74] suggested that FA-based activated concrete has a 1.15% loss in mass when soaked in 5% H2SO4 solutions. Results revealed that the incorporation of RHA and CSP increases the acid resistance compared to specimens with 90% slag. However, RHA has a better effect than CSP. This may be accredited to the existence of $Ca(OH)_2$. Mixtures with 40 % RHA possessed a weight loss of less than 1.5% at 180 days of exposure, see Figure 14. This conforms with Kim et al. [37] who specified that alkali-activated concrete blinded with RHA had exceptional acid resistance. It should be noted that most samples demonstrate insignificant changes in color in the H2SO4 solution. As for the residual compressive strength, results revealed all mixtures suffer a reduction in CS, this is in agreement with previous researchers [75]. This is attributed to the breakdown of C-A-S-H and the expansion occurred due to the formation of gypsum forming extra cracks allowing for more deterioration. However, results reveal that increasing the CSP decreases the loss of compressive strength, see Figure 15.

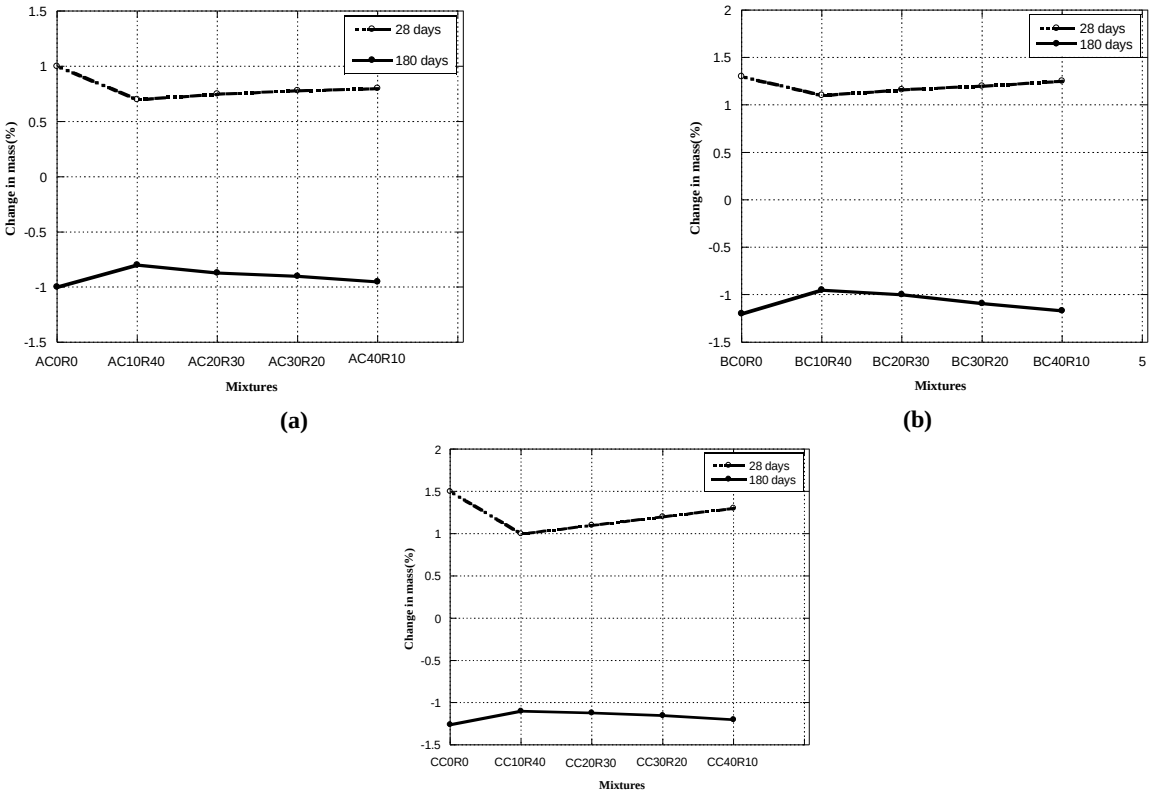


**Figure13: Percentage of change in mass at 28 and 180 days, (a) Mix A, (b) Mix B, (c) Mix C**

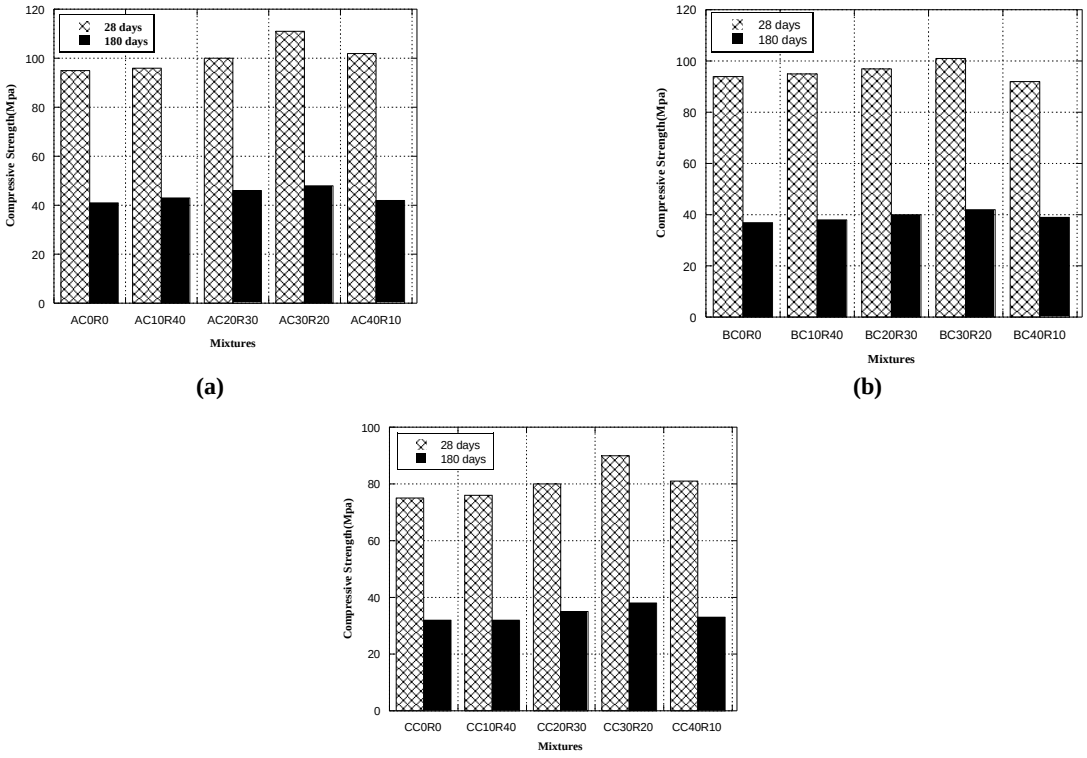


**Figure 14: Compression strength for mixtures subjected to H2SO4, Mix A, (b) Mix B, (c) Mix**

## 5 CONCLUSIONS

The following conclusions are yielded:

1. The workability increases as the CSP content increases competed to slag-based GPC.
2. The strength analysis revealed that CSP decreases strength in the early stage due to the lower CaO content. However, improvement in strength was observed in the later stage due to the participation of active silica in the reaction.
3. The combination of CSP/RHA improves the mechanical properties competed to slag-based GPC.
4. The CSP/RHA addition to slag/FA GPC produced high strength concrete without elevated curing temperature.
5. The use of a combination of CSP/RHA up to 50% improves the durability of GPC exposed to sulfuric acid attack, carbonation, and chloride attack. This is accredited to reduced gypsum formation and low porosity.

## 6 RECOMMENDATIONS FOR FUTURE WORK

Attempts should be exerted to have geopolymers that can be simply mixed in the field of construction. More additives should be originated to help attain higher early strength at ambient temperature curing. Thorough analyses are necessary to allow geopolymer to be an alternative to Portland.

**Acknowledgments**

N/A

**Availability of data and material**

The data that supports the findings of this study are available in the supporting information of this article.

**Competing interests**

The authors declare that they have no known competing financial interests or personal relationships.

**Funding**

Self-funding is applied.

## REFERENCES

1. Keshavarz, Z. and Mostofinejad, D. "Porcelain and red ceramic wastes used as replacements for coarse aggregate in concrete," Construction and Building Material, vol. 195, 2009, pp.218-230, https://doi.org/10.1016/j.conbuildmat.2018.11.033.
2. Amin, M., Tayeh, B. A. and Agwa, I. S. "Effect of using mineral admixtures and ceramic wastes as coarse aggregates on properties of ultrahigh-performance concrete," Journal of Cleaner Production, vol. 273, 2020, https://doi.org/10.1016/j.jclepro.2020.123073.
3. Mohammad Hosseini, H.; Lim, N.H.A.S.; Tahir, M.M.; Alyousef, R.; Alabduljabbar, H.; Samadi, M. "Enhanced performance of green mortar comprising high volume of ceramic waste in aggressive environments", Construction and Building Materials, vol. 212, 2019, pp. 607–617, DOI: 10.1016/j.conbuildmat.2019.04.024
4. U.S. Beemamol, A. and Nizad, M. Nazeer. "Investigations on cement mortar using ceramic tailing sand as fine aggregate," American Journal of Engineering Research, 2013, pp. 28–33.
5. Khartabil, A. and Martini, S. Al. "Carbonation resistance of sustainable concrete using recycled aggregate and supplementary cementitious materials," Key Engineering Materials, vol. 803, 2019, pp.246-252, https://doi.org/10.4028/www.scientific.net/KEM.
6. Keppert, M., Vejmelková, E., Bezdička, P., Doleželová, M., Čáchová, M., Scheinherrová, L., Pokorný, J., Vyšvařil, M., Rovnaníková, and P. and Černý, R. "Red-clay ceramic powders as geopolymer precursors: Consideration of amorphous portion and CaO content," Applied Clay Science. vol. 161, 2018, pp. 82-89, https://doi.org/10.1016/j.clay.2018.04.019
7. Kermeli, K., Edelenbosch, O. Y., Crijns-Graus, W., van Ruijven, B. J., Mima, S., van Vuuren, D. P. and Worrell, E. "The scope for better industry representation in long-term energy models: Modeling the cement industry," Applied Energy, vol. 240, 2019, pp. 964-985, https://doi.org/10.1016/j.apenergy.2019.01.252
8. Lee, H. S., Lim, S. M. and Wang, X. Y. "Optimal Mixture Design of Low-CO2 High-Volume Slag Concrete Considering Climate Change and CO2 Uptake," International Journal of Concrete Structures and Materials, vol. 13, 2019, https://doi.org/10.1186/s40069-019-0359-7
9. Kim, T. H., Tae, S. H., Suk, S. J., Ford, G. and Yang, K. H. "An optimization system for concrete life cycle cost and related CO2 emissions," Sustainability, vol. 8, 2016, pp. 361, https://doi.org/10.3390/su8040361
10. Miller, S. A., John, V. M., Pacca, S. A. and Horvath, A. "Carbon dioxide reduction potential in the global cement industry by 2050," Cement and Concrete Research, vol. 114, 2018, pp. 115-124, https://doi.org/10.1016/j.cemconres.2017.08.026
11. Ahmad, M. R., Das, C. S., Khan, M. and Dai, J. G. "Development of low-carbon alkali-activated materials solely activated by flue gas residues (FGR) waste from incineration plants," Journal of Cleaner Production, vol. 397, 2023, https://doi.org/10.1016/j.jclepro.2023.136597
12. Shah, V. and Bishnoi, S. "Carbonation resistance of cements containing supplementary cementitious

materials and its relation to various parameters of concrete. Construction and Building Materials, vol. 178, 2018, pp. 219-232, https://doi.org/10.1016/j.conbuildmat.2018.05.162
13. Han-Seung, L., and Wang, X. Y. "Evaluation of compressive strength development and carbonation depth of high-volume slag-blended concrete," Construction and Building Materials, vol. 124, 2016, pp. 45-54, https://doi.org/10.1016/j.conbuildmat.2016.07.070
14. Bouaissi A., Li L.-Y., Abdullah M.M.A.B., and Bui Q.-B. "Mechanical properties and microstructure analysis of FA-GGBS-HMNS based geopolymer concrete," Construction and Building Materials, vol. 210, 2019, pp. 198–209, doi: 10.1016/j.conbuildmat.2019.03.202.
15. Li, O. H., Yun-Ming, L., Cheng-Yong, H., Bayuaji, R., Abdullah, M. M. A. B., Loong, F. K., Jin, T. S., Teng, N. H., Nabiałek, M., Jeż, B. and Sing, N. Y. "Evaluation of the effect of silica fume on amorphous fly ash geopolymers exposed to elevated temperature," Magnetochemistry, vol. 7, 2021, https://doi.org/10.3390/magnetochemistry7010009
16. Li, Y., Shen, J., Lin, H. and Li, Y. "Optimization design for alkali-activated slag-fly ash geopolymer concrete based on artificial intelligence considering compressive strength, cost, and carbon emission," Journal of Building Engineering, vol. 75, 2023, https://doi.org/10.1016/j.jobe.2023.106929
17. Faris, M. A., Abdullah, M. M. A. B., Muniandy, R., Hashim, M. F. A., Błoch, K., Jeż, B., Garus, S., Palutkiewicz, P., Mortar, N. A. M. and Ghazali, M. F. "Comparison of hook and straight steel fibers addition on Malaysian fly ash-based geopolymer concrete on the slump, density, water absorption and mechanical properties," Materials, vol. 14, 2021, https://doi.org/10.3390/ma14051310
18. Luhar, S., Cheng, T. W., and Luhar, I. "Incorporation of natural waste from agricultural and aquacultural farming as supplementary materials with green concrete: A review," In Composites Part B: Engineering, vol. 175, 2019, https://doi.org/10.1016/j.compositesb.2019.107076
19. Luhar, S., Cheng, T. W., Nicolaides, D., Luhar, I., Panias, D. and Sakkas, K. "Valorisation of glass wastes for the development of geopolymer composites – Durability, thermal and microstructural properties: A review," Construction and Building Materials, vol. 222, 2019, pp. 673-687, https://doi.org/10.1016/j.conbuildmat.2019.06.169
20. Shaikh, F. U. A., Luhar, S., Arel, H. Ş. and Luhar, I. "Performance evaluation of Ultrahigh performance fibre reinforced concrete – A review," Construction and Building Materials, vol. 232, 2020, https://doi.org/10.1016/j.conbuildmat.2019.117152
21. Van Deventer, J. S. J., Provis, J. L., Duxson, P. and Brice, D. G. "Chemical research and climate change as drivers in the commercial adoption of alkali activated materials," Waste and Biomass Valorization, vol. 1, 2010, pp. 145-155, https://doi.org/10.1007/s12649-010-9015-9.
22. Haque, F., Fan, C., and Lee, Y. Y. "From waste to value: Addressing the relevance of waste recovery to agricultural sector in line with circular economy," Journal of Cleaner Production, vol. 415, 2023, https://doi.org/10.1016/j.jclepro.2023.137873
23. Yinfei, D., Wei, H., Mingxin, D. and Weizheng, L. "Using silicon carbide to increase thermal conductivity of cement composite for improving heating efficiency of floor heating system," Construction and Building Materials, vol. 325, 2022, https://doi.org/10.1016/j.conbuildmat.2022.126707
24. M. Ibrahim, M. Maslehuddin, "An overview of factors influencing the properties of alkali-activated binders", Journal of Cleaning Production, vol. 286, 2021, https://doi.org/10.1016/j.jclepro.2020.124972
25. Kou, Y., Jiang, H., Ren, L., Yilmaz, E., and Li, Y. "Rheological properties of cemented paste backfill with alkali-activated slag," Minerals, vol. 10, 2020, https://doi.org/10.3390/min10030288
26. Salami, B. A., Ibrahim, M., Algaifi, H. A., Alimi, W. and Ewebajo, A. O. "A review on the durability performance of alkali-activated binders subjected to chloride-bearing environment," Construction and Building Materials, vol. 317, 2022, https://doi.org/10.1016/j.conbuildmat.2021.125947
27. Abbass, A. M., Elrahman, M. A., Abdel-Gawwad, H. A. and Stephan, D. "Critical parameters affecting the thermal resistance of alkali-activated aluminosilicate wastes: Current understanding and future directions," Environmental Science and Pollution Research, vol. 30, 2023, pp.84874-84897, https://doi.org/10.1007/s11356-023-28336-9
28. Yu, M., Lin, H., Wang, T., Shi, F., Li, D., Chi, Y. and Li, L. yuan. "Experimental and numerical investigation on thermal properties of alkali-activated concrete at elevated temperatures" Journal of Building Engineering," vol. 74, 2023, https://doi.org/10.1016/j.jobe.2023.106924
29. Heikal, M., Zaki, M. E. A., and Ibrahim, S. M. Preparation, physico-mechanical characteristics and durability of eco-alkali-activated binder from blast-furnace slag, cement kiln-by-pass dust and microsilica ternary system," Construction and Building Materials, vol. 260, 2020, https://doi.org/10.1016/j.conbuildmat.2020.119947
30. Al-Otaibi, S. "Durability of concrete incorporating GGBS activated by waterglass," Construction and Building Materials, vol. 22, 2008, pp. 2059-2067, https://doi.org/10.1016/j.conbuildmat.2007.07.023

31. Ossama M. Mohamed. "Effects of the Curing Regime, Acid Exposure, Alkaline Activator Dosage, and Precursor Content on the Strength Development of Mortar with Alkali-Activated Slag and Fly Ash Binder: A Critical Review," Polymers, vol. 15, 2023, https://doi.org/10.3390/polym15051248
32. Khater, H. M. "Effect of silica fume on the characterization of the geopolymer materials," International Journal of Advanced Structural Engineering, vol. 5, 2013, https://doi.org/10.1186/2008-6695-5-12
33. Bernal, S. A., Mejía De Gutiérrez, R., Pedraza, A. L., Provis, J. L., Rodriguez, E. D. and Delvasto, S. "Effect of binder content on the performance of alkali-activated slag concretes," Cement and Concrete Research, vol. 41, 2011, pp.1-8, https://doi.org/10.1016/j.cemconres.2010.08.017
34. Saptamongkol, A., Sata, V., Wongsa, A., Kroehong, W., Ekprasert, J. and Chindaprasirt, P. "Hybrid geopolymer paste from high calcium fly ash and glass wool: Mechanical, microstructure, and sulfuric acid and magnesium sulfate resistance characteristics," Journal of Building Engineering, vol. 76, 2023, https://doi.org/10.1016/j.jobe.2023.107245
35. El-Feky, M. S., Kohail, M., El-Tair, A. M. and Serag, M. I. "Effect of microwave curing as compared with conventional regimes on the performance of alkali activated slag pastes," Construction and Building Materials, vol. 233, 2020, https://doi.org/10.1016/j.conbuildmat.2019.117268
36. Rashad, A. M. "Properties of alkali-activated fly ash concrete blended with slag," Iranian Journal of Materials Science and Engineering, vol. 10, 2013, pp. 57-64.
37. Y.Y. Kim, B.-J. Lee, V. Saraswathy, S.-J. Kwon, "Strength and durability performance of alkali-activated rice husk ash geopolymer mortar", The Scientific World Journal, 2014, https://doi.org/10.1155/2014/209584
38. Li, X., Yang, Z., Yang, S., Zhang, K., and Chang, J. "Synthesis process-based mechanical property optimization of alkali-activated materials from red mud: A review," Journal of Environmental Management, vol. 344, 2023, https://doi.org/10.1016/j.jenvman.2023.118616
39. Chen, M. C., Fang, W., Xu, K. C. and Xie, L. "Research on Durability of Recycled Ceramic Powder Concrete," IOP Conference Series Materials Science and Engineering, vol. 216, 2017, https://doi.org/10.1088/1757-899X/216/1/012018
40. Viramgama, P. D., Vaniya, P. S. R. and Parikh, P. K. B. "Effect of ceramic waste powder in self-compacting concrete properties: A critical review," IOSR Journal of Mechanical and Civil Engineering, vol. 13, 2016, pp. 08-13.
41. Huseien, G. F., Sam, A. R. M., Shah, K. W. and Mirza, J. "Effects of ceramic tile powder waste on properties of self-compacted alkali-activated concrete," Construction and Building Materials, vol. 236, 2020, https://doi.org/10.1016/j.conbuildmat.2019.117574
42. Aly, S. T., Kanaan, D. M., El-Dieb, A. S. and Abu-Eishah, S. I. "Properties of Ceramic Waste Powder-Based Geopolymer Concrete," In International Congress on Polymers in Concrete (ICPIC 2018), pp.429-435, https://doi.org/10.1007/978-3-319-78175-4_54
43. Azevedo, A. R. G., Vieira, C. M. F., Ferreira, W. M., Faria, K. C. P., Pedroti, L. G. and Mendes, B. C. "Potential use of ceramic waste as precursor in the geopolymerization reaction for the production of ceramic roof tiles," Journal of Building Engineering, vol. 29, 2020, https://doi.org/10.1016/j.jobe.2019.101156
44. Saxena, R. and Gupta, T. "Assessment of mechanical, durability and microstructural properties of geopolymer concrete containing ceramic tile waste," Journal of Material Cycles and Waste Management, vol. 24, 2022, pp. 725-742, https://doi.org/10.1007/s10163-022-01353-5
45. Rashad, A. M. and Essa, G. M. F. "Effect of ceramic waste powder on alkali-activated slag pastes cured in hot weather after exposure to elevated temperature," Cement and Concrete Composites, vol. 111, 2020, https://doi.org/10.1016/j.cemconcomp.2020.103617
46. Zhang, G. Y., Bae, S. C., Lin, R. S. and Wang, X. Y. "Effect of waste ceramic powder on the properties of alkali–activated slag and fly ash pastes exposed to high temperature.," Polymers, vol. 13, 2021, https://doi.org/10.3390/polym13213797
47. Shoaei, P., Musaeei, H. R., Mirlohi, F., Narimani zamanabadi, S., Ameri, F. and Bahrami, N. "Waste ceramic powder-based geopolymer mortars: Effect of curing temperature and alkaline solution-to-binder ratio," Construction and Building Materials, vol. 227, 2019, https://doi.org/10.1016/j.conbuildmat.2019.116686
48. ASTM. (2014). Astm C618. Annual Book of ASTM Standards.
49. ASTM Committee C09.91. (2015). ASTM C125-15a Standard Terminology Relating to Concrete and Concrete Aggregates. In Annual Book of ASTM Standards Volume 04.02.
50. ASTM. (2015). ASTM C143/C143M-12 Standard Test Method for Slump of Hydraulic-Cement Concrete. Annual Book of ASTM Standards.

51. Zareei, S. A., Ameri, F., Shoaei, P. and Bahrami, N. "Recycled ceramic waste high strength concrete containing wollastonite particles and micro-silica: A comprehensive experimental study," Construction and Building Materials, vol. 201, 2019, pp. 11-32, https://doi.org/10.1016/j.conbuildmat.2018.12.161
52. ASTM C 496/C 496M. (2011). Standard Test Method for Splitting Tensile Strength of Cylindrical Concrete Specimens. ASTM International.
53. ASTM (2018). "Standard Test Method for Flexural Strength of Concrete (Using Simple Beam with Third-Point Loading)." ASTM C78, ASTM International, West Conshohocken, PA.
54. ASTM C1585. (2013). ASTM C1585: Standard Test Method for Measurement of Rate of Absorption of Water by Hydraulic - Cement Concretes. Annual Book of ASTM Standards.
55. ASTM International. (2021). ASTM C642-21. Standard Test Method for Density, Absorption, and Voids in Hardened Concrete. In ASTM International.
56. ASTM I American Society for Testing and Materials. (1997). Astm C 1202. ASTM International.
57. American Society for Testing and Materials. (2007). ASTM C596-07 Standard Test Method for Drying Shrinkage of Mortar Containing Hydraulic Cement. Annual Book of ASTM Standards Volume 04.01.
58. Huseien, G. F., Sam, A. R. M., Shah, K. W., Asaad, M. A., Tahir, M. M. and Mirza, J. "Properties of ceramic tile waste-based alkali-activated mortars incorporating GBFS and fly ash., "Construction and Building Materials, vol. 214, 2019, https://doi.org/10.1016/j.conbuildmat.2019.04.154
59. Suraneni, P., Burris, L., Shearer, C. R. and Hooton, R. D., ASTM C618 Fly Ash Specification: Comparison with Other Specifications, Shortcomings, and Solution, vol. 118, 2021, https://doi.org/10.14359/51725994
60. Nath, P. and Sarker, P. K. "Effect of GGBFS on setting, workability and early strength properties of fly ash geopolymer concrete cured in ambient condition," Construction and Building Materials, vol. 66, 2014, pp. 163-171, https://doi.org/10.1016/j.conbuildmat.2014.05.080
61. Ma, B., Zhu, Z., Huo, W., Yang, L., Zhang, Y., Sun, H.and Zhang, X. "Assessing the viability of a high performance one-part geopolymer made from fly ash and GGBS at ambient temperature," Journal of Building Engineering., vol. 75, 2023, https://doi.org/10.1016/j.jobe.2023.106978
62. Rivera, J. F., Cristelo, N., Fernández-Jiménez, A. and Mejía de Gutiérrez, R. "Synthesis of alkaline cements based on fly ash and metallurgic slag: Optimisation of the SiO 2 /Al 2 O 3 and Na 2 O/SiO 2 molar ratios using the response surface methodology," Construction and Building Materials, vol. 213, 2019, pp. 424-433, https://doi.org/10.1016/j.conbuildmat.2019.04.097
63. Hwang, C. L., Damtie Yehualaw, M., Vo, D. H. and Huynh, T. P. "Development of high-strength alkali-activated pastes containing high volumes of waste brick and ceramic powders," Construction and Building Materials, vol. 218, 2019, pp. 519-529, https://doi.org/10.1016/j.conbuildmat.2019.05.143
64. Bouaissi, A., Li, L. yuan, Al Bakri Abdullah, M. M. and Bui, Q. B. "Mechanical properties and microstructure analysis of FA-GGBS-HMNS based geopolymer concrete," Construction and Building Materials, vol. 210, 2019, pp. 198-209, https://doi.org/10.1016/j.conbuildmat.2019.03.202
65. Deb, P. S., Nath, P., and Sarker, P. K. "The effects of ground granulated blast-furnace slag blending with fly ash and activator content on the workability and strength properties of geopolymer concrete cured at ambient temperature," Materials and Design, vol. 62, 2014, pp.32-39, https://doi.org/10.1016/j.matdes.2014.05.001
66. Achak, H., Sohrabi, M. R. and Hoseini, S. O. "Effects of microsilica and polypropylene fibers on the rheological properties, mechanical parameters and durability characteristics of green self-compacting concrete containing ceramic wastes," Construction and Building Materials, vol. 392, 2023, https://doi.org/10.1016/j.conbuildmat.2023.131890
67. Visairo-Méndez, R., Torres-Acosta, A. A. and Alvarado-Cárdenas, R. "Durability performance indices for cement-based mortars," Materials, vol. 14, 2021, https://doi.org/10.3390/ma14112758
68. Aziz, I. H., Al Bakri Abdullah, M. M., Mohd Salleh, M. A. A., Yoriya, S., Chaiprapa, J., Rojviriya, C., and Li, L. Y. "Microstructure and porosity evolution of alkali activated slag at various heating temperatures," Journal of Materials Research and Technology, vol. 9, 2020, pp. 15894-15907, https://doi.org/10.1016/j.jmrt.2020.11.041
69. Asadi, I., Shafigh, P., Abu Hassan, Z. F. Bin, and Mahyuddin, N. B. "Thermal conductivity of concrete – A review," Journal of Building Engineering, vol. 20, 2018, pp. 81-93, https://doi.org/10.1016/j.jobe.2018.07.002
70. Asadi I., Shafigh P., Hassan Z.F.B.A., Mahyuddin N.B. "Thermal conductivity of concrete–A review," Journal of Building Engineering, vol. 20, 2018, pp. 81–93. doi: 10.1016/j.jobe.2018.07.002.
71. Huseien, G. F., Ismail, M., Tahir, M. M., Mirza, J., Khalid, N. H. A., Asaad, M. A., Husein, A. A., and Sarbini, N. N. "Synergism between palm oil fuel ash and slag: Production of environmental-friendly alkali activated mortars with enhanced properties,"

Construction and Building Materials, vol. 170, 2018, https://doi.org/10.1016/j.conbuildmat.2018.03.031

72. Gui-Yu Zhang, Yong-Han Ahn, Run-Sheng Lin, and Xiao-Yong Wang, "Effect of Esaste Ceramic Powder on Properties of Alkali-Activated Blast Furnace Slag Paste and Mortar", Polymers, vol. 13, 2021, https://doi.org/10.3390/ polym13162817
73. Shagñay, S., Garcia-Lodeiro, I., Velasco, F., Bautista, A., and Torres-Carrasco, M. "Mineralogical and microstructural changes in alkali-activated and hybrid materials exposed to accelerated leaching," Journal of Building Engineering, vol. 64, 2023, https://doi.org/10.1016/j.jobe.2022.105733
74. M. Malviya, H.S. Goliya, "Durability of fly ash based geopolymer concrete using alkaline solutions (NaOH and Na2SiO3)," International Journal of Emergency Trends, vol. 6, 2014, pp. 18–33.
75. PanelJun Liu, Renjie Niu, Junjie Hu, Yuanrui Ren, Weizhuo Zhang, Guang Liu, Zhenlin Li, Feng Xin g, Jie Ren. The performance and microstructure of alkali-activated artificial aggregates prepared from municipal solid waste incineration bottom ash. Construction and Building Materials, 403, 2023, https://doi.org/10.1016/j.conbuildmat.2023.133012